

The Infrared Spectrum of Uranium Hollow Cathode Lamps from 850 nm to 4000 nm: Wavenumbers and Line Identifications from Fourier Transform Spectra

Stephen L. Redman^{1,2}, James E. Lawler³, Gillian Nave², Lawrence W. Ramsey^{1,4}, Suvrath Mahadevan^{1,4}

ABSTRACT

We provide new measurements of wavenumbers and line identifications of 10 100 UI and UII near-infrared (NIR) emission lines between 2500 cm^{-1} and $12\,000\text{ cm}^{-1}$ (4000 nm to 850 nm) using archival FTS spectra from the National Solar Observatory (NSO). This line list includes isolated uranium lines in the Y, J, H, K, and L bands ($0.9\text{ }\mu\text{m}$ to $1.1\text{ }\mu\text{m}$, $1.2\text{ }\mu\text{m}$ to $1.35\text{ }\mu\text{m}$, $1.5\text{ }\mu\text{m}$ to $1.65\text{ }\mu\text{m}$, $2.0\text{ }\mu\text{m}$ to $2.4\text{ }\mu\text{m}$, and $3.0\text{ }\mu\text{m}$ to $4.0\text{ }\mu\text{m}$, respectively), and provides six times as many calibration lines as thorium in the NIR spectral range. The line lists we provide enable inexpensive, commercially-available uranium hollow-cathode lamps to be used for high-precision wavelength calibration of existing and future high-resolution NIR spectrographs.

Subject headings: atomic spectra, Fourier transform spectroscopy, near infrared, uranium, wavelengths

1. Introduction

Astronomical spectrographs are used for a variety of high-precision measurements, ranging from the discovery of low mass exoplanets (Mayor et al. 2009) to the possible variation of fundamental constants, such as the fine structure constant (Webb et al. 2001) or the proton-electron mass ratio (Malec et al. 2010). These works require excellent wavelength calibration sources and a detailed understanding of the associated uncertainties and systematics. In the era of extremely large telescopes (ELTs) it is often the accuracy of the calibration source, not the intrinsic photon

¹Department of Astronomy & Astrophysics, The Pennsylvania State University, University Park, PA 16802

²National Institute of Standards and Technology, Gaithersburg, MD 20899

³Department of Physics, University of Wisconsin, 1150 University Avenue, Madison, WI 53706

⁴Center for Exoplanets and Habitable Worlds, The Pennsylvania State University, University Park, PA 16802

noise, that limits the achievable precision. Furthermore, the science goals of future ELTs will require very high-precision calibration sources. Below 900 nm, the well-established thorium-argon (Th/Ar) hollow cathode lamps have been a workhorse (Palmer & Engleman 1983). Continual improvements in the line list have now enabled Th lamps to be used to calibrate almost the entire optical bandpass with high precision (Lovis & Pepe 2007; Murphy et al. 2007).

In contrast to the optical, the near infrared (NIR) does not yet have a widely-used calibrator like Th/Ar (see Mahadevan & Ge (2009) for a detailed discussion). Kerber et al. (2008) have provided an atlas of Th/Ar lines in the NIR, which is sufficient for precisions of ≈ 50 m/s on CRIRES (CRyogenic high-resolution InfraRed echelle Spectrograph) (Kaeufl et al. 2004), but the density of Th lines is relatively low in the NIR, and many of the thorium lines are very weak. Better precisions of 6 m/s to 10 m/s have been achieved by Figueira et al. (2010) with Telluric CO₂ lines, and 5 m/s by Bean et al. (2010) with an ammonia (NH₃) gas cell in the K band. Such calibration techniques are suitable for specific problems, but are only useful over specific ranges of the NIR.

An ideal emission calibration source would cover the observed spectrum in a forest of isolated lines of similar intensity, with the intrinsic wavelength of each line known to a high degree of precision. Laser frequency combs are such a calibration source (Murphy et al. 2007; Osterman et al. 2007; Braje et al. 2008; Quinlan et al. 2010), but there are numerous technical hurdles before these systems will be considered turn-key: they are expensive to build and operate, they have yet to demonstrate the long-term stability and desired wavelength coverage for the NIR. Hollow cathode lamps, being significantly less expensive and easier to use, are the preferred wavelength calibration solution for most astrophysical spectrographs. We refer the reader to Kerber et al. (2007) for a comprehensive review of the design, construction, and operation of hollow cathode lamps. Thorium (²³²Th), an element often used as the cathode for such lamps, exhibits many of the desired characteristics of an atomic emission calibration source: it has many energy levels (leading to many lines), a heavy nucleus, a very long half-life, and occurs in nature as a single isotope. Uranium shares all of these characteristics except for the last: it has three naturally-occurring isotopes, the major component being uranium-238 (99.275%), with much smaller amounts of uranium-235 (0.720%) and uranium-234 (0.005%) (Rosman & Taylor 1998). These isotopes could limit the achievable precision, but the second-most abundant isotope, uranium-235, has hyperfine structure, so the fine structure transitions are spread over several lines and are thus much less intense. For practical purposes, all of the uranium lines are observed as “single” lines in the FTS spectra. In this paper we propose an inexpensive and simple solution to the calibration problem in the NIR: the use of uranium hollow cathode lamps, which provide a high density of emission lines across the NIR spectral region.

Prior works have noted that uranium might prove a higher line density calibration source than thorium (Engleman 2003). Experiments with a variety of metals and fill gases in hollow

cathode lamps on the Pathfinder spectrographic testbed (Ramsey et al. 2008; Ramsey et al. 2010) between 1 μm and 1.6 μm confirms this. Figure 1 shows 25-second exposures of Th/Ar, U/Ar, and U/Ne obtained with Pathfinder. All lamps were run at 14 mA and share the same optical alignment. In addition to the greater line density of uranium lines, we note that neon lines in our U/Ne spectra are much less intense than argon lines in our U/Ar spectra. These results are typical for our observations in the NIR.

Using archival Fourier transform spectrometer (FTS) data from the Kitt Peak National Solar Observatory (hereafter, NSO), we have identified 10 100 uranium lines between 0.85 μm and 4 μm , most of which are below 2 μm . This line list complements work by Palmer et al. (1980), who provided uranium identifications for bright uranium lines from 26 000 cm^{-1} down to 11 000 cm^{-1} (3846 \AA to 9091 \AA), and Conway et al. (1984), who compiled a list of uranium lines between 1.8 μm and 5.5 μm . Our goal is to provide the astrophysical community with a list of largely unblended wavelength standards that can be used for the calibration of current and future NIR spectrographs.

In §2 we describe the archival FTS data from which we derived our measurements and line lists, and in §3 we describe the construction of the line lists, and the determination of uncertainties. In §4 we present the results of this line list, and in §5 we compare our line list to historical uranium line lists and to recent thorium line lists. In §6 we summarize our conclusions.

2. Fourier-Transform Spectra

The observations used for our measurements were made with the 1-m FTS on Kitt Peak (Brault 1976) between 1979 and 2002, and are publicly available on the NSO website¹. We selected two high-current U/Ar spectra taken with InSb detectors, two low-current U/Ar spectra to check for plasma shifts, and one high-current U/Ne spectrum to search for lines above 9000 cm^{-1} . Plasma shifts in this paper refer to line shifts from some combination of effects including: collisions with neutral atoms, electrons, and ions, and Stark effect due to static electric fields, and in the case of ion lines the Doppler effect due to ion drift motion. A summary of these data can be found in Table 1. The first column is the spectrum number (shorthand which is used throughout the text). The second column is the name of the archive data file (the first six digits indicate the year, month, and day of the observations, respectively, and the last three indicate the spectrum number of that day). The third column is the lamp type (either uranium neon or uranium argon). Column four is the lamp current in milliamps (mA). The wavenumber range of the observation is given in the next two columns. Column seven is the wavenumber correction factor (κ , defined below) applied

¹http://diglib.nso.edu/nso_user.html

to each spectrum, and column eight is the standard error of the mean in that factor (both divided by 10^{-7} for readability).

These data were reduced and analyzed using the interactive computer program XGREMLIN, which is an X-windows implementation of Brault’s GREMLIN program (Brault & Abrams 1989) that was developed by Griesmann (Nave et al. 1997). The earlier uranium interferograms (SP3, SP4, and SP5) were taken with unequal numbers of points on each side of the zero path difference and the line profiles in the corresponding spectra have large, antisymmetric imaginary parts. Such spectra require careful phase correction in order to ensure that none of the imaginary part of the line profile is rotated into the real part, causing a dispersion-shaped instrumental profile (Learner et al. 1995). We re-transformed SP4 and SP5 from the original interferograms in order to confirm that the phase correction was done correctly. In all cases, the residual phase errors were less than 20 mrad, corresponding to a maximum wavenumber shift of 0.0003 cm^{-1} .

Independent data reductions of SP5 were carried out by two of us (Redman and Lawler). In these approaches, lines were kept if they appeared in both SP4 and SP5, had a S/N ratio above 10, and were symmetric and had a consistent width. Numerical derivatives (Redman) or integrals (Lawler) were used to determine the center-of-gravity wavenumbers. In regions where these independent reductions overlapped, matching wavenumbers (within 0.01 cm^{-1}) were averaged with equal weighting. 97% of the lines identified via these independent analyses were within 0.002 cm^{-1} of each other. Where SP4 and SP5 wavenumbers matched within 0.01 cm^{-1} , they were averaged, with twice as much weight given to the higher-current spectrum SP5.

A thermal continuum is observed in our spectra in the wavelength region above $1.5 \mu\text{m}$. This was subtracted from the spectra. All lines with a signal-to-noise ratio of at least 10 in SP4 and SP5 and 20 in SP3 were then found in these spectra. Voigt profiles were fitted to these lines to obtain the wavenumber, peak intensity, line width, and Voigt line shape parameters. Since spectrum SP3

Table 1: NSO FTS Observations

Spectrum Number	Archive Filename	Species	Current (mA)	Wavenumber (cm^{-1})		κ ($/10^{-7}$)	$\delta\kappa$ ($/10^{-7}$)
				Start	End		
SP1	020227.023	U/Ar	26	3900	14400	2.13	0.66
SP2	020227.024	U/Ar	26	4100	14400	2.09	0.64
SP3	790221.005	U/Ne	75	8300	22200	-4.62	0.54
SP4	820520.003	U/Ar	169	1800	9300	-6.38	0.83
SP5	801214.005	U/Ar	300	2400	9500	-15.08	0.82

Notes. Uranium-argon and uranium-neon FTS spectra from the NSO Archive.

was taken in air, all wavenumbers in this spectrum were converted to vacuum wavenumbers with the formulae of Edlén (1966) using the pressure, temperature, and humidity in the header. We estimate residual errors in the wavenumbers from this correction to be less than 0.0004 cm^{-1} . We also calculated these wavenumbers using equation 3 of Peck & Reeder (1972), but found the wavenumbers differed from those obtained with the Edlén formula by less than a factor of 4 parts in 10^9 .

The wavenumber scale of a FTS is linear and is defined by the control laser used to measure the optical path difference in the interferometer. However, differences in the optical path through the FTS between the laser and the lamp beam result in a small stretching or compression of the wavenumber scale. This effect can be corrected by measuring the wavenumbers of standard lines throughout the spectrum and using them to calculate a multiplicative wavenumber correction factor, κ_i , using

$$\kappa_i = \frac{\sigma_{\text{std},i}}{\sigma_{\text{obs},i}} - 1 \quad (1)$$

where $\sigma_{\text{obs},i}$ is the wavenumber of a line observed in the spectrum and $\sigma_{\text{std},i}$ is the wavenumber of that line, based on an independent wavelength calibration. The wavenumber correction factor for the spectrum κ is calculated from the weighted mean of the κ_i s. All the wavenumbers in the spectrum are multiplied by $(1 + \kappa)$ to put them on an absolute scale. Measurements of κ for spectra SP3 and SP5 can be seen in Figure 2. The legend quotes the trimmed mean (including only points that lie within three standard deviations of the mean κ) of κ for each species, along with an uncertainty that is the sum of the standard error of the mean and the uncertainties of the absolute calibrants.

Wavenumber standards for the calibration of our spectra were taken from three references: Ar I lines from Whaling et al. (2002) measured using an FTS, Ne lines from Sansonetti et al. (2004) measured using an FTS, and eight U lines from Degraffenreid & Sansonetti (2002) measured using laser spectroscopy. The Ar I wavenumbers of Whaling et al. (2002) have been shown to be too large by 6.7 parts in 10^8 by Sansonetti (2007). Wavenumbers of Ar I lines are also susceptible to plasma shifts, but Kerber et al. (2008) showed that these shifts are less than 0.0003 cm^{-1} (3 parts in 10^7) for Ar I lines with upper levels less than $115\,000 \text{ cm}^{-1}$. We thus calibrated spectra SP1, SP2, SP4 and SP5 with Ar I lines with upper levels below $115\,000 \text{ cm}^{-1}$ using wavenumbers taken from Whaling et al. (2002), with the correction of Sansonetti (2007).

The uranium lines of Degraffenreid & Sansonetti (2002) appear in spectra SP1, SP2 and SP3, but cover a small wavenumber range between 13269 cm^{-1} and 14391 cm^{-1} . The calibration of SP1 and SP2 using these lines agrees with the calibration using Ar I lines to 7 parts in 10^8 , which is within the combined uncertainties for spectrum SP2. Spectrum SP3 contains the uranium lines of

Degraffenreid & Sansonetti (2002) and neon lines of Sansonetti et al. (2004). The neon standards, however, show a slope in the correction factor of about 2 parts in 10^7 between 9000 cm^{-1} and $14\,000\text{ cm}^{-1}$. Since we observe similar slopes on other uranium/neon spectra we studied during selection of the five spectra we have chosen for this work, we believe this slope is present in the neon lines of Sansonetti et al. (2004) and not in spectrum SP3. The calibrated uranium lines of SP3 agree with those measured in spectra SP1 and SP2 within the joint uncertainties (See Figure 2). Therefore, we used only the uranium lines from Degraffenreid & Sansonetti (2002) to calibrate spectrum SP3.

We went through each spectrum individually to check and make sure each feature identified by XGremLin was indeed a line and not a ghost or ringing. Some of these features were expurgated by modeling the measured uranium line widths (as a function of wavenumber) with a second-order polynomial, and measuring the standard deviation of those line widths. Potential uranium lines or unidentified lines with line widths greater than or less than three standard deviations from this polynomial fit were culled from the line list. An example of this is given in Figure 3. We realize that this technique likely eliminated highly-blended uranium lines, but this is perfectly in line with our goals, since these blended lines cannot be used for precise wavelength calibration.

A relative radiometric calibration of the intensities in Table 2 was performed to convert all intensities to a relative photon flux. The SP3 and SP5 radiometric calibrations are based on tungsten strip lamp spectra recorded shortly before or after the uranium data and (in the case of SP5) on the relative intensities of ArI lines embedded in the uranium hollow cathode lamp spectra. The tungsten strip lamp was calibrated as a spectral radiance standard above 6500 cm^{-1} . Below this, we estimated the spectrum using a 2400-K blackbody curve. We confirmed our calibration by measuring relative intensities of ArI lines in our spectrum and comparing them to published branching ratios (Whaling et al. 1993). During the data analysis we did not observe any self reversed lines. The extraordinarily rich energy level structure of neutral and ionized U tends to suppress optical depth errors in the relative intensities of Table 2, even at relatively high lamp currents.

3. Line List Construction

The quality of spectrum SP5 was noticeably better than spectrum SP3 (which had a lower S/N) and spectrum SP4 (which exhibited spurious ringing around bright lines of an unknown origin), and we therefore elected to weight this spectrum twice as much as these spectra. This line list was first matched to known argon lines from Whaling et al. (2002) or neon lines from Sansonetti et al. (2004), depending on the source, within a 0.01 cm^{-1} window. To identify the uranium lines, we first calculated possible transition wavenumbers from energy level differences (Ritz wavenumbers) us-

ing the database of actinides², which are based upon Blaise & Radziemski (1976) and Blaise et al. (1994). Since these Ritz wavenumbers are based on a least-squares adjustment of all of the lines, the impact of blended lines is minimized. All lines were compared to these energy level transitions using the same 0.01 cm^{-1} window function. Uranium and Noble gas lines were distinguished primarily based upon the line widths.

After this initial identification procedure, roughly 30% of the lines had more than one possible classification. Many of these multiple classifications are incorrect. They occur because the high density of spectral lines and energy levels in the uranium spectrum gives rise to many spurious coincidences between measured wavenumbers and energy level differences. The classifications of each of these lines was examined to determine the most probable classification. The primary criterion was the agreement between the observed wavenumber and the wavenumber derived from the energy levels (the Ritz wavenumber). For this to be a useful criterion, accurate energy levels are needed. The majority of the energy levels from Blaise & Radziemski (1976) and Blaise et al. (1994) match our spectra within 0.001 cm^{-1} . For some levels, the difference between the observed and Ritz wavenumbers was much larger. In these cases, a consistent difference was found for all the lines from the upper level, indicating that the value of the energy level was not consistent with our data. Although better agreement would be obtained by optimizing the energy levels to our data, our spectra do not cover a sufficiently large wavenumber region for an optimization of all uranium energy levels. We have thus used the energy levels from the database of the actinides without adjustment. An additional criterion for the acceptance of a classification of a line was the energy of the upper level of the transition. The majority of the lines in our spectra have upper energy levels below $35\,000 \text{ cm}^{-1}$ and strong lines usually have upper levels at even lower energies. After sorting our line list in this way, very few (205) lines have more than one possible classification.

3.1. Uncertainties

The uncertainty of a measured line position is a combination of the uncertainty in the measurement and the uncertainty in the standard lines used to set the wavelength scale. Typically, these two measurements have been treated as if they are independent of each other, so that they are added in quadrature. However, the uncertainty of the standard lines usually consist of two components: a statistical component, which is the standard deviation of the measurements, and a systematic component, which is common to all of the standard lines (e.g., the standard error of the mean of the original calibration of the standard lines). The systematic component is usually small, but can accumulate to a non-trivial level if the lines are calibrated with numerous intermediary standards.

²<http://www.lac.u-psud.fr/Database/Tab-energy/Uranium/U-el-dir.html>

In such a case, these measurements are not statistically independent, and should be added together linearly rather than in quadrature. As such, we have chosen to add our uncertainties linearly.

The weighted uncertainty in the wavenumber correction factor of a particular spectrum ($\delta_{SPX,\kappa}$) is given by:

$$\delta_{SPX,\kappa} = \sqrt{\frac{1}{\sum_{i=1}^N \frac{1}{\delta_{\kappa,i}^2}}} + \left\langle \frac{\delta_{std,i}}{\sigma_{std,i}} \right\rangle \quad (2)$$

where the first term is the standard error of the mean of the measured wavenumber correction factors, and the second term is the mean of the ratio of the uncertainty in the wavenumber of the standard, $\delta_{std,i}$, and the wavenumber of the standards, $\sigma_{std,i}$. The weighting factor is based on the uncertainty of each of the individual measurements of κ_i :

$$\delta_{\kappa,i} = \sqrt{\left(\frac{\partial \kappa}{\partial \sigma_{std,i}}\right)^2 \delta_{std,i}^2 + \left(\frac{\partial \kappa}{\partial \sigma_{obs,i}}\right)^2 \delta_{lc,i}^2} \quad (3)$$

where $\delta_{std,i}$ is the uncertainty in the line from the literature, and $\delta_{lc,i}$ is the statistical uncertainty of the line center:

$$\delta_{lc,i} = \frac{W_i}{S/N_i} \quad (4)$$

where W_i is the width of the line, and S/N_i is the signal-to-noise ratio of the line. This equation is derived from equation 9.2 in Davis et al. (2001), assuming only one statistically-independent point in a line width, which is typical for our under-sampled spectra.

In a given spectrum SPX, the uncertainty in the wavenumber of a line i is the sum of the statistical uncertainty (Equation 4) and the uncertainty in the wavenumber correction factor:

$$\delta_{SPX,i} = \sigma_{obs,i} \delta_{SPX,\kappa} + \frac{W_i}{S/N_i} \quad (5)$$

When a line was found in multiple spectra, these spectrum-specific uncertainties were added in inverse quadrature:

$$\delta_i = \left(\frac{1}{\delta_{SPX,i}^2} + \frac{1}{\delta_{SPY,i}^2} + \dots \right)^{-\frac{1}{2}} \quad (6)$$

4. Results

The complete table of uranium lines is several hundred pages long, and is available in the electronic version of this publication. A short selection of the complete list is presented in Table 2 to aid in interpretation of the machine-readable (ASCII) table.

The first column is the weighted mean wavenumber, in cm^{-1} , with twice as much weight given to the line position measurements of spectrum SP5 than to spectra SP3 or SP4. The second column is the combined standard uncertainty in the wavenumber measurement (as outlined in § 3.1, in 10^{-3}cm^{-1}). The third and fourth columns are the corresponding vacuum wavelength and wavelength uncertainties. The fifth column lists the calibrated intensity of the spectral features. The sixth column provides the species identification, and ionization state for uranium lines. A “?” in this column indicates that the line does not fall within 0.01cm^{-1} of a possible uranium transition based on Ritz wavenumbers, but that is most likely uranium, based on the line width. The next four columns are the upper and lower energy levels for uranium transitions. The eleventh column is the difference between the Ritz energy level transition and the observed wavenumber of the line. The last column provides notes on the particular lines; lines that exhibit noticeable asymmetries are denoted with a **bl** to indicate that they appear to be blended at the resolution of the FTS.

Table 2. Uranium Line List Sample

Wavenumber (cm ⁻¹)	Wavenumber	Wavelength nm	Wavelength	Relative Photon Flux	Species	Upper		Lower		$\sigma_{Ritz} - \langle \sigma \rangle$ (10 ⁻³ cm ⁻¹)	Notes
	Uncertainty (10 ⁻³ cm ⁻¹)		Uncertainty pm			Energy (cm ⁻¹)	J	Energy (cm ⁻¹)	J		
6467.6270	1.1	1546.1621	0.3	3.35	?						
6467.8736	0.5	1546.1032	0.1	33.59	UII	15812	7/2	9344	5/2	1.4	
6468.2394	0.9	1546.0157	0.2	6.38	UII	19097	11/2	12629	13/2	-1.4	
6468.9299	0.6	1545.8507	0.2	86.08	UI	23560	4	17091	3	1.1	
6469.7201	1.1	1545.6619	0.3	2.38	UI	27150	8	20680	7	-1.1	
6470.1238	0.6	1545.5655	0.2	16.26	UI	24535	5	18065	5	0.2	
6470.2048	1.6	1545.5461	0.4	3.32	UII	22868	9/2	16397	11/2	0.2	
					UI	30443	2	23973	3	-0.8	
6470.2715	0.9	1545.5302	0.2	3.87	UI	21329	7	14858	7	-0.5	
6470.9276	0.6	1545.3735	0.1	49.91	UI	34086	5	27615	6	3.4	
6471.4221	0.6	1545.2554	0.1	16.93	UI	22377	5	15906	6	1.9	bl
6471.5367	0.9	1545.2280	0.2	4.12	UI	18260	2	11788	3	1.3	
6471.6477	1.6	1545.2015	0.4	2.72	UII	24923	13/2	18451	13/2	0.3	
6471.8228	0.6	1545.1597	0.1	36.65	UI	23932	5	17461	5	0.2	
6472.0924	0.6	1545.0954	0.1	64.63	Ar						

Notes. A small example of the uranium line list. The classifications are given for UI and UII lines, as are the offsets from the Ritz energy level differences. Lines unassociated with known uranium level transitions are identified as a “?”. These lines are likely also uranium lines, based on their narrow line widths. A **bl** in the last column indicates a line which appears to be blended at the resolution of the FTS.

Although it is tempting to convert our data to emission branching fractions for various upper levels which decay primarily in the IR, we strongly argue that the reader resist doing so for the following reasons. First, we did not perform the calibration, and cannot be assured of its validity (although we believe the header data to be accurate). Second, our intensity calibration is less reliable below 6500 cm^{-1} , where we used a 2400-K blackbody curve and ArI branching fractions to estimate the tungsten strip spectrum beyond its measured range. Third, any branching fractions deduced solely from this work will be incomplete, because we only analyze the IR. At the very least, some additional tests are desirable. Specifically, a check for possible optical depth errors on some of the strongest emission lines to low lying levels should be performed by re-measuring their branching ratios over a range of lamp currents.

The physical conditions of the plasma inside the hollow cathode lamp can shift the spectral lines systematically. Such shifts are found by comparing data taken under a variety of conditions. We compared the lines from our low-current observations (SP1 & SP2) to the lines of our highest-current observation (SP5). No systematic plasma shifts were observed at the 10^{-3} cm^{-1} level (see Figure 4).

In all, we identified 8991 UI lines and 1150 UII lines. 1244 lines remain unidentified, but are likely to be UI or UII, based on their narrow line widths. We see no uranium-235 lines in our spectra, both because of the relatively low abundance of this isotope, and because hyperfine structure lowers the intensity of these lines relative to uranium-238.

To assist with the use of this line list in the H band, we have constructed an atlas of uranium-neon lines between $14\,540\text{ \AA}$ and $16\,380\text{ \AA}$. This atlas was measured at a resolution of $50\,000$ using Pathfinder, and independently calibrated with a laser frequency comb. The U/Ne hollow cathode lamp was run at 14 mA. Measurements of the spectral peaks of these lines show excellent agreement with the FTS-measured wavenumbers in this publication. This spectroscopic atlas will be published separately (Redman et al. in preparation).

5. Comparison with Other Uranium and Thorium Line Lists

Our line list overlaps those of Palmer et al. (1980) between $11\,000\text{ cm}^{-1}$ and $12\,000\text{ cm}^{-1}$, and of Conway et al. (1984) between 2500 cm^{-1} and 5500 cm^{-1} . A comparison of our wavenumbers is shown in Figure 5. All the wavenumbers of Palmer & Engleman are $(0.75 \pm 0.53) \times 10^{-3}\text{ cm}^{-1}$ greater than ours. Palmer et al. (1980) did not calibrate their spectra with standard lines and the only corrections they made to their wavenumber scale were due to the refractive index of air and the finite aperture of the FTS. This likely accounts for the difference between our two wavenumber scales. That being said, their estimated uncertainties overlap our measurements within one or two

standard deviations. Several outliers are low-S/N lines near bright lines, and as such are difficult to measure. Our measurements of these lines differ slightly from those of Palmer et al. (1980), but these lines are likely to not be very useful for high-precision calibration anyway.

The comparison to Conway et al. (1984) (bottom frame of Fig. 5) is on the same scale and shows a much larger scatter. This is not surprising, considering their measurements have an order of magnitude less precision than our own measurements. Even so, our measurements agree to within $(1.26 \pm 0.80) \times 10^{-3} \text{ cm}^{-1}$.

The top plot in Figure 6 shows a histogram comparing the population density of uranium lines from this work and thorium lines from Kerber et al. (2008). Note that the lamp used in the latter was run at 20 mA, much less than the lamp currents of the FTS uranium observations, so more thorium lines undoubtedly exist in the NIR that have not yet been published. The difference in quantity between this line list and Kerber’s excellent Th/Ar work is quantified in Table 3. The gap in the uranium line density around 9250 cm^{-1} is an artifact of the spectral response function of the archival data used to create this line list, and not representative of the true number of uranium lines in this region. The response functions of spectra SP5 and SP3 are plotted in this same panel, and are based upon tungsten strip lamp spectra taken under the same observing conditions as their corresponding uranium spectra.

The bottom plot in Figure 6 shows a comparison between the number of neon and argon lines in the same spectral region (bottom). As shown in Fig. 1, not only are the neon lines less numerous, they are also much fainter than argon lines in the same spectral region.

6. Conclusions

We have measured 10 100 uranium lines in the NIR, which represents a significant increase in the number of calibration lines over the current NIR emission standard, Th/Ar. This line list has been generated specifically with astronomical applications in mind — we have taken care to avoid blended lines, and where we could not do so, we have indicated suspected or likely blends in the table. We anticipate this line list will be useful on several upcoming astronomical spectrographs, including APOGEE (Allende Prieto et al. 2008), CARMENES (Quirrenbach et al. 2010), and iSHELL (Tokunaga et al. 2008).

7. Acknowledgements

We acknowledge support from NASA through grant NNX10AN93G and the NAI and Origins grant NNX09AB34G, and the NSF grant AST 1006676. Financial support is provided by NSF under Grant AST-0906034 and NIST. This research was partially performed while SLR held a National Research Council Research Associateship Award at NIST. This work was partially supported by funding from the Center for Exoplanets and Habitable Worlds. The Center for Exoplanets and Habitable Worlds is supported by the Pennsylvania State University, the Eberly College of Science, and the Pennsylvania Space Grant Consortium. We would also like to thank Joe Reader, John Curry, Florian Kerber, and the anonymous referee for carefully reading the paper and providing useful feedback.

REFERENCES

- Allende Prieto, C., Majewski, S., Schiavon, R., Cunha, K., Frinchaboy, P., Holtzman, J., Johnston, K., Shetrone, M., Skrutskie, M., Smith, V., et al. 2008, *Astronomische Nachrichten*, 329, 1018
- Bean, J. L., Seifahrt, A., Hartman, H., Nilsson, H., Wiedemann, G., Reiners, A., Dreizler, S., & Henry, T. J. 2010, *ApJ*, 713, 410
- Blaise, J. & Radziemski, Jr., L. J. 1976, *Journal of the Optical Society of America (1917-1983)*, 66, 644
- Blaise, J., Wyart, J., Vergès, J., Engleman, Jr., R., Palmer, B. A., & Radziemski, L. J. 1994, *Journal of the Optical Society of America B Optical Physics*, 11, 1897
- Braje, D. A., Kirchner, M. S., Osterman, S., Fortier, T., & Diddams, S. A. 2008, *Eur. Phys. J. D*, 48, 57
- Brault, J. & Abrams, M. 1989, *OSA Technical Digest Series (Washington: Optical Society of America)*, 6, 110
- Brault, J. W. 1976, *Journal of the Optical Society of America (1917-1983)*, 66, 1081
- Conway, J. G., Worden, E. F., Brault, J. W., Hubbard, R. P., & Wagner, J. J. 1984, *Atomic Data and Nuclear Data Tables*, 31, 299
- Davis, S., Abrams, M., & Brault, J. 2001, *Fourier Transform Spectrometry (Academic, New York, 2001)*

- Degraffenreid, W. & Sansonetti, C. J. 2002, *Journal of the Optical Society of America B Optical Physics*, 19, 1711
- Edlén, B. 1966, *Metrologia*, 2, 71
- Engleman, Jr., R. 2003, *J. Quant. Spec. Radiat. Transf.*, 78, 1
- Figueira, P., Pepe, F., Melo, C. H. F., Santos, N. C., Lovis, C., Mayor, M., Queloz, D., Smette, A., & Udry, S. 2010, *A&A*, 511, A55+
- Kaeufl, H., Ballester, P., Biereichel, P., Delabre, B., Donaldson, R., Dorn, R., Fedrigo, E., Finger, G., Fischer, G., Franza, F., et al. 2004, *Proc. SPIE* 5492, 1218–1227
- Kerber, F., Nave, G., & Sansonetti, C. 2008, *The Astrophysical Journal Supplement Series*, 178, 374
- Kerber, F., Nave, G., Sansonetti, C., Bristow, P., & Rosa, M. 2007, in *ASP Conf. Ser.*, Vol. 364, 461
- Learner, R. C. M., Thorne, A. P., Wynne-Jones, I., Brault, J. W., & Abrams, M. C. 1995, *Journal of the Optical Society of America A*, 12, 2165
- Lovis, C. & Pepe, F. 2007, *A&A*, 468, 1115
- Mahadevan, S. & Ge, J. 2009, *ApJ*, 692, 1590
- Malec, A. L., Buning, R., Murphy, M. T., Milutinovic, N., Ellison, S. L., Prochaska, J. X., Kaper, L., Tumlinson, J., Carswell, R. F., & Ubachs, W. 2010, *Monthly Notices of the Royal Astronomical Society*, 403, 1541
- Mayor, M., Bonfils, X., Forveille, T., Delfosse, X., Udry, S., Bertaux, J., Beust, H., Bouchy, F., Lovis, C., Pepe, F., Perrier, C., Queloz, D., & Santos, N. C. 2009, *A&A*, 507, 487
- Murphy, M. T., Udem, T., Holzwarth, R., Sismann, A., Pasquini, L., Araujo-Hauck, C., Dekker, H., D’Odorico, S., Fischer, M., Hänsch, T. W., & Manescau, A. 2007, *MNRAS*, 380, 839
- Nave, G., Sansonetti, C., & Griesmann, U. 1997, *Fourier Transform Spectroscopy: Methods and Applications*, 3, 38
- Osterman, S., Diddams, S., Beasley, M., Froning, C., Hollberg, L., MacQueen, P., Mbele, V., & Weiner, A. 2007, in *Society of Photo-Optical Instrumentation Engineers (SPIE) Conference Series*, Vol. 6693, *Society of Photo-Optical Instrumentation Engineers (SPIE) Conference Series*, 66931G–1–9

- Palmer, B., Keller, R., & Engleman Jr, R. 1980, Atlas of uranium emission intensities in a hollow cathode discharge, Tech. rep., LA-8251-MS, Los Alamos Scientific Lab., NM (USA)
- Palmer, B. A. & Engleman, R. 1983, Atlas of the Thorium spectrum, ed. Palmer, B. A. & Engleman, R.
- Peck, E. R. & Reeder, K. 1972, *Journal of the Optical Society of America* (1917-1983), 62, 958
- Quinlan, F., Ycas, G., Osterman, S., & Diddams, S. A. 2010, *Rev. Sci. Instrum.*, 81, 063105
- Quirrenbach, A., Amado, P. J., Mandel, H., Caballero, J. A., Mundt, R., Ribas, I., Reiners, A., Abril, M., Aceituno, J., Afonso, C., Barrado Y Navascues, D., Bean, J. L., Béjar, V. J. S., Becerril, S., Böhm, A., Cárdenas, M. C., Claret, A., Colomé, J., Costillo, L. P., Dreizler, S., Fernández, M., Francisco, X., Galadí, D., Garrido, R., González Hernández, J. I., Guàrdia, J., Guenther, E. W., Gutiérrez-Soto, F., Joergens, V., Hatzes, A. P., Helmling, J., Henning, T., Herrero, E., Kürster, M., Laun, W., Lenzen, R., Mall, U., Martin, E. L., Martín-Ruiz, S., Mirabet, E., Montes, D., Morales, J. C., Morales Muñoz, R., Moya, A., Naranjo, V., Rabaza, O., Ramón, A., Rebolo, R., Reffert, S., Rodler, F., Rodríguez, E., Rodríguez Trinidad, A., Rohloff, R. R., Sánchez Carrasco, M. A., Schmidt, C., Seifert, W., Setiawan, J., Solano, E., Stahl, O., Storz, C., Suárez, J. C., Thiele, U., Wagner, K., Wiedemann, G., Zapatero Osorio, M. R., Del Burgo, C., Sánchez-Blanco, E., & Xu, W. 2010, in *Society of Photo-Optical Instrumentation Engineers (SPIE) Conference Series*, Vol. 7735, Society of Photo-Optical Instrumentation Engineers (SPIE) Conference Series
- Ramsey, L., Barnes, J., Redman, S., Jones, H., Wolszczan, A., Bongiorno, S., Engel, L., & Jenkins, J. 2008, *Publications of the Astronomical Society of the Pacific*, 120, 887
- Ramsey, L. W., Mahadevan, S., Redman, S., Bender, C., Roy, A., Zonak, S., Sigurdsson, S., & Wolszczan, A. 2010, in *Society of Photo-Optical Instrumentation Engineers (SPIE) Conference Series*, Vol. 7735, Society of Photo-Optical Instrumentation Engineers (SPIE) Conference Series, 773571–1–6
- Redman, S. L., Ycas, G. G., Terrian, R., Mahadevan, S., Ramsey, L. W., Bender, C. F., Osterman, S. N., Diddams, S. A., Quinlan, F., Lawler, J. E., & Nave, G. in preparation
- Rosman, K. & Taylor, P. 1998, *Journal of Physical and Chemical Reference Data*, 27, 1275
- Sansonetti, C. 2007, *Journal of Research of the National Institute of Standards and Technology*, 112, 297
- Sansonetti, C., Blackwell, M., & Saloman, E. 2004, *Journal of Research — National Institute of Standards and Technology*, 109, 371

Tokunaga, A. T., Bond, T., Jaffe, D. T., Mumma, M. J., Rayner, J. T., Tollestrup, E. V., & Warren, D. W. 2008, in Society of Photo-Optical Instrumentation Engineers (SPIE) Conference Series, Vol. 7014, Society of Photo-Optical Instrumentation Engineers (SPIE) Conference Series

Webb, J. K., Murphy, M. T., Flambaum, V. V., Dzuba, V. A., Barrow, J. D., Churchill, C. W., Prochaska, J. X., & Wolfe, A. M. 2001, Physical Review Letters, 87, 091301

Whaling, W., Anderson, W., Carle, M., Brault, J., & Zarem, H. 2002, Journal of Research — National Institute of Standards and Technology, 107, 149

Whaling, W., Carle, M. T., & Pitt, M. L. 1993, J. Quant. Spec. Radiat. Transf., 50, 7

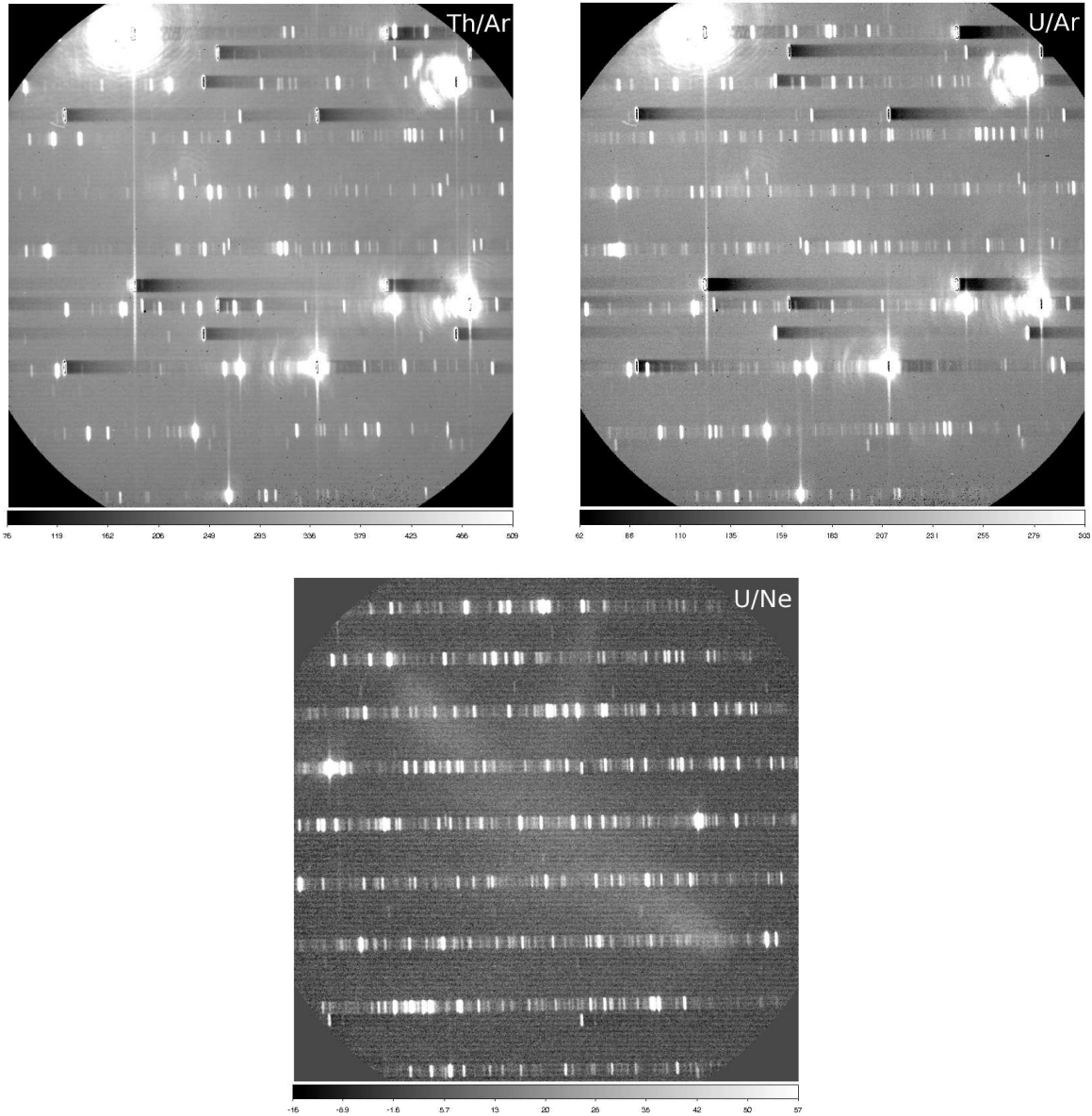


Fig. 1.— Y-band observations with the Pathfinder spectrograph (Ramsey et al. 2008; Ramsey et al. 2010) of Th/Ar (top-left), U/Ar (top-right) and U/Ne (bottom). All lamps were run at 14 mA through the same optical alignment, and all three images are the median-average of twenty-five 25-second exposures. Thus, lines common between the top exposures are argon, etc. The scale of each image is shown at the bottom of each image, and has been adjusted to bring out the faintest lines. Note the much higher background present in the Ar images; bright argon lines mask out the fainter actinides. Multiplexer cross-talk is responsible for the negative images of bright lines in adjacent quadrants. Neon provides a much cleaner image; the faint inter-order scattered light pattern in the U/Ne exposure (visible as a set of faint diagonal streaks) is from three relatively bright neon lines in spectral orders not present on the array.

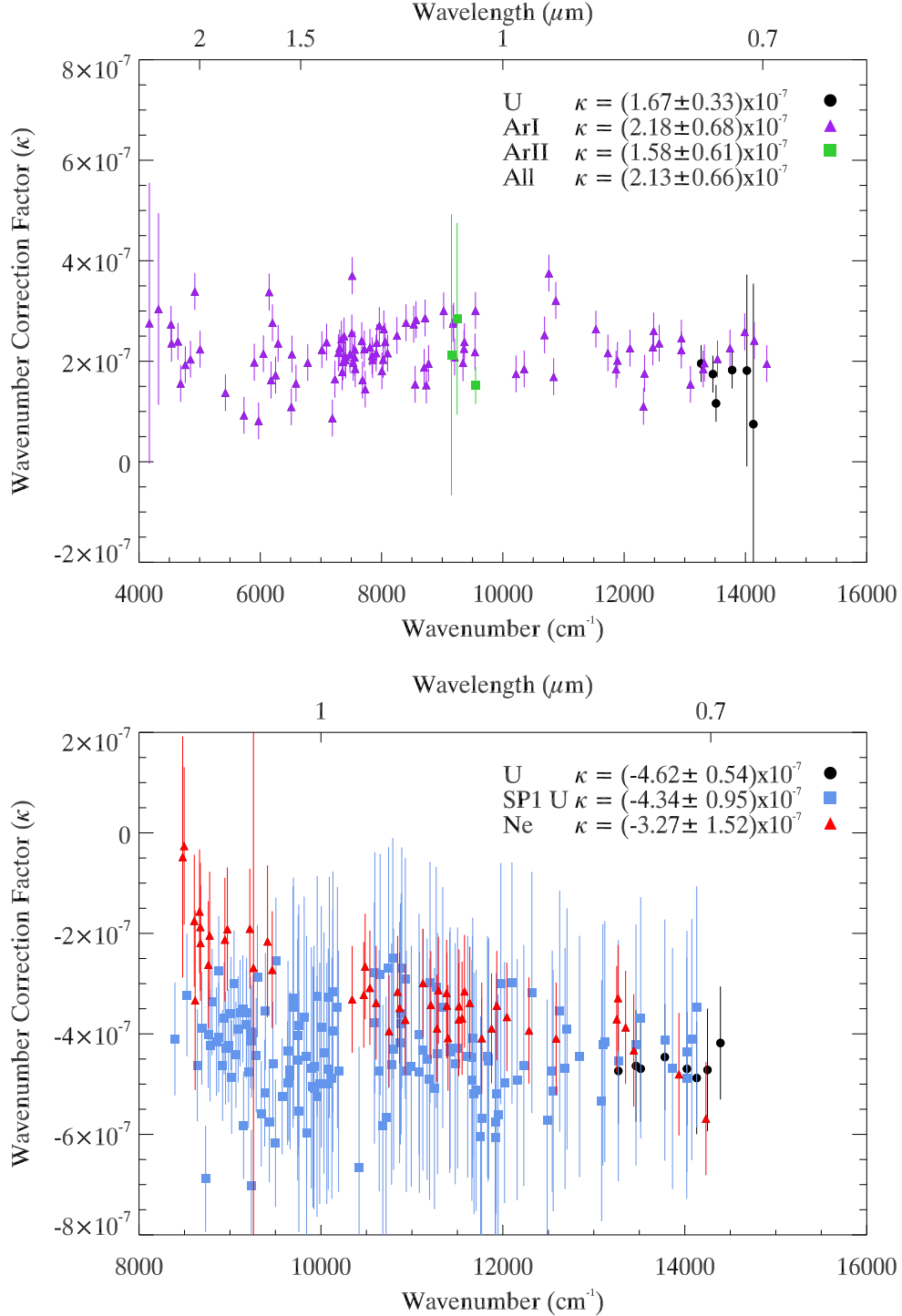


Fig. 2.— **Top:** Wavenumber correction factor of SP1, using wavenumber standards from Whaling et al. (2002); Sansonetti (2007) (ArI and ArII lines) and Degraffenreid & Sansonetti (2002) (U lines). Uncertainties in this plot are calculated via Equation 3. **Bottom:** The same, but for SP3 (U/Ne). The neon standards come from Sansonetti et al. (2004), and a comparison to the uranium lines of SP1 are from this work.

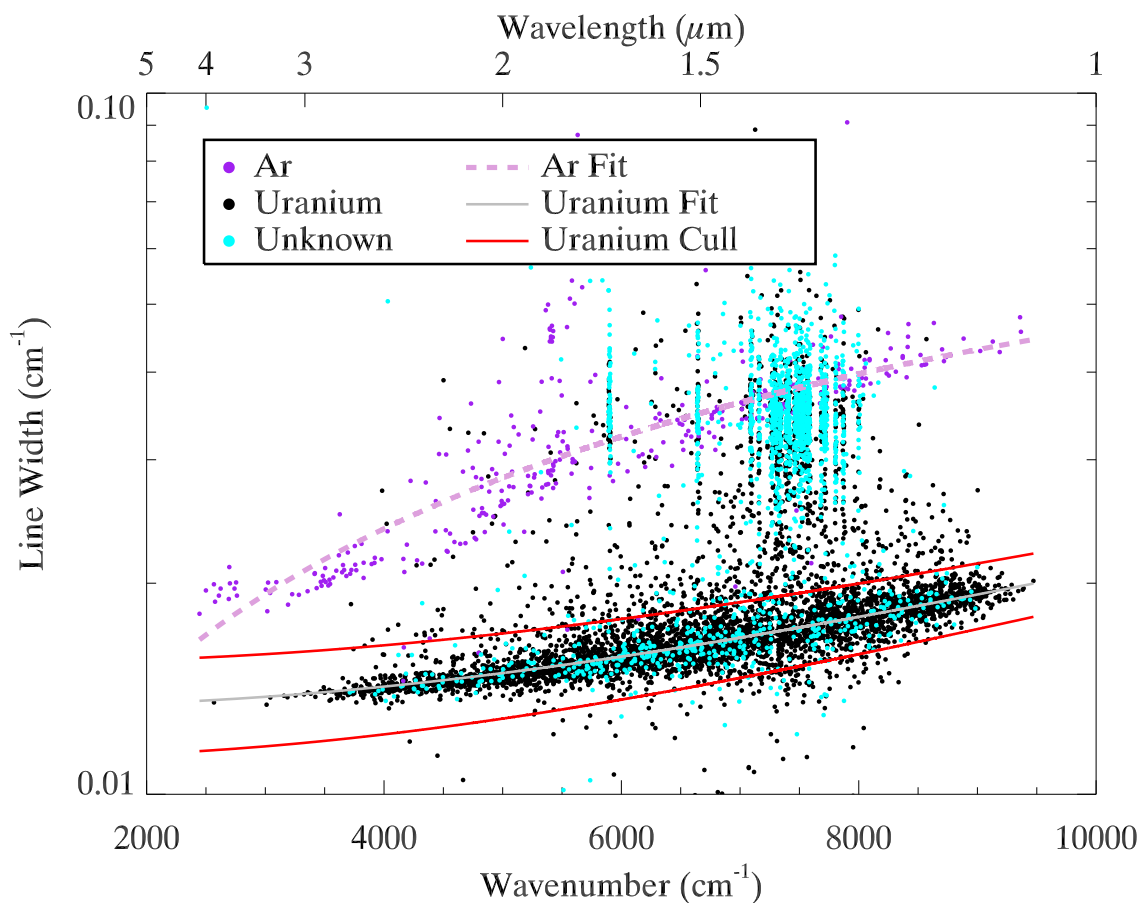


Fig. 3.— A diagnostic plot showing how we first culled blended lines and spurious features from SP5. Argon lines are wider than uranium lines, and these line widths increase gradually with increasing wavenumber. These changes are well-fit by a second-order polynomial (gray line for uranium, pink dashed line for argon). Potential uranium lines with line widths more than three standard deviations from this fit (red lines) were culled from the list. Approximately 24% of all potential uranium lines were culled in this manner. This technique also removes blended uranium lines from our line list, which are not as useful for precise wavelength measurements.

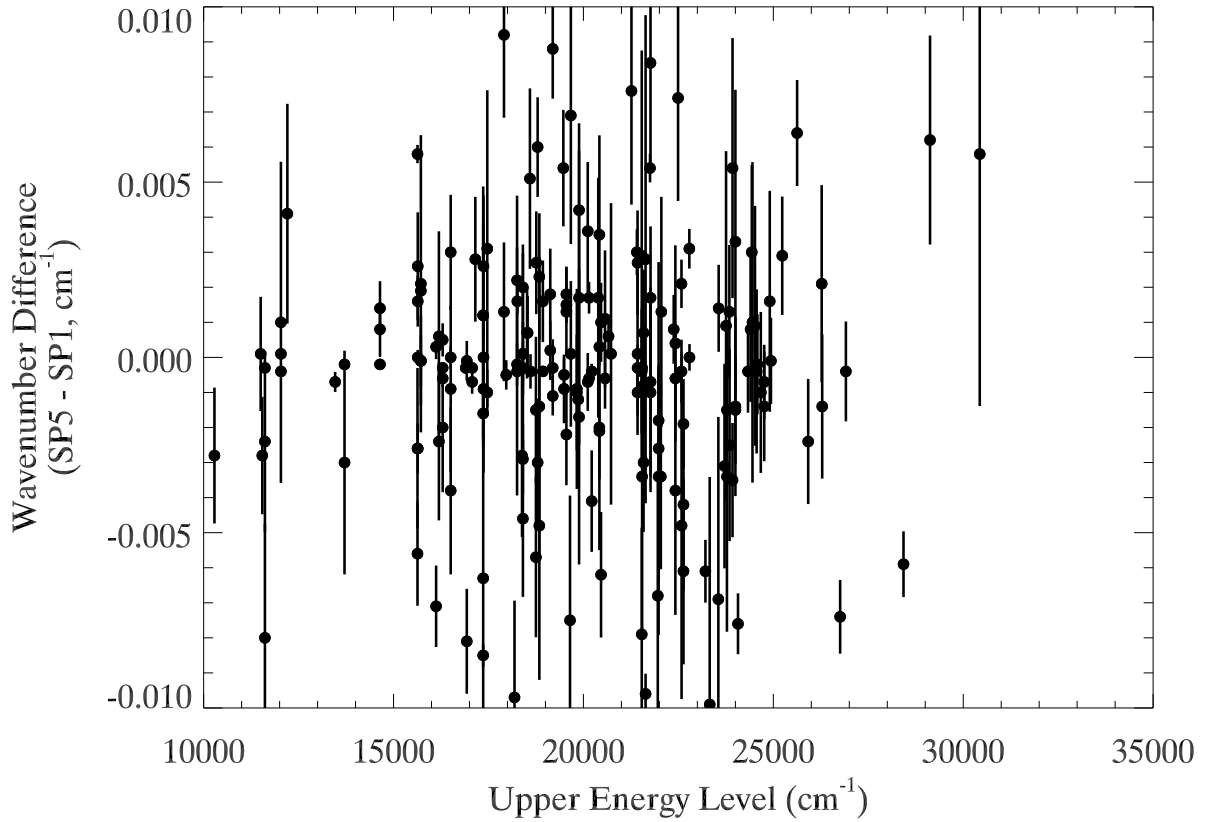


Fig. 4.— The wavenumber difference (in cm^{-1}) between our highest-current spectrum (SP5, 300 mA) and our lowest-current spectrum (SP1, 26 mA) as a function of the upper energy level of the transition. The uncertainties are the sum in quadrature of the uncertainties in SP1 and SP5. The lack of a trend indicates that plasma shifts are not an issue for these upper energy levels.

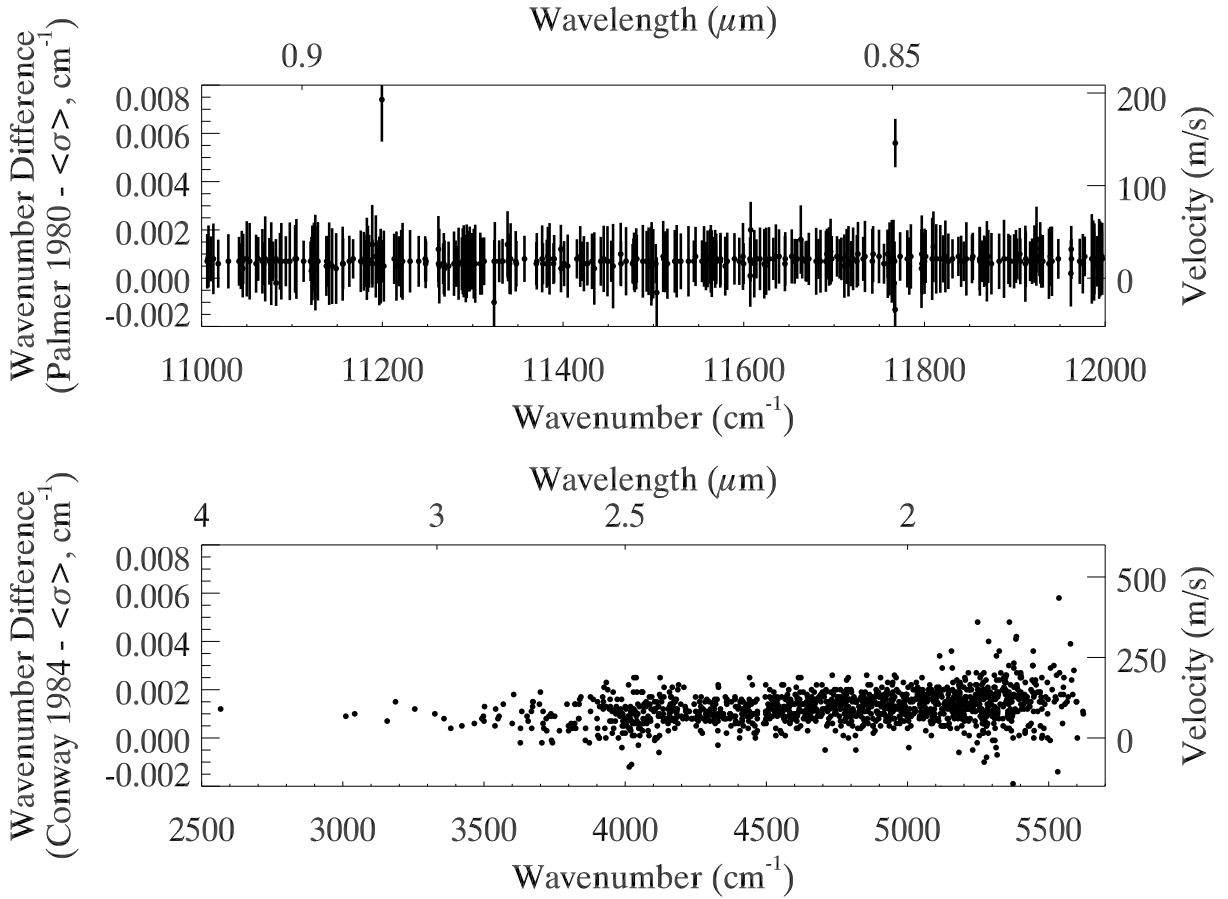


Fig. 5.— Comparisons to historical uranium line lists. **Top:** A comparison to the lines of Palmer et al. (1980). The average offset and one standard deviation of this offset is $(0.75 \pm 0.53) \times 10^{-3} \text{ cm}^{-1}$. The equivalent velocity offset and single standard deviation (using the central wavenumber) is $(20 \pm 14) \text{ m/s}$. The fact that the statistical deviation between the two data sets is smaller than the estimated uncertainty for most lines indicates that Palmer et al. (1980) did a good job estimating the uncertainty of their uncalibrated data. Some outliers are weak lines near bright, unresolved uranium lines (which exhibit ringing); these lines are difficult to measure, and our measurements differ slightly from those of Palmer et al. (1980). **Bottom:** A comparison to the lines of Conway et al. (1984). The average offset and one standard deviation of this offset is $(1.26 \pm 0.80) \times 10^{-3} \text{ cm}^{-1}$. Error bars in each are the sum in quadrature of our uncertainties and the uncertainties of the aforementioned authors. In the case of Conway et al. (1984), we have omitted the error bars for readability; the average error bar in this case is $\pm 0.001 \text{ cm}^{-1}$. The equivalent velocity offset and single standard deviation (using the central wavenumber) is $(57 \pm 36) \text{ m/s}$.

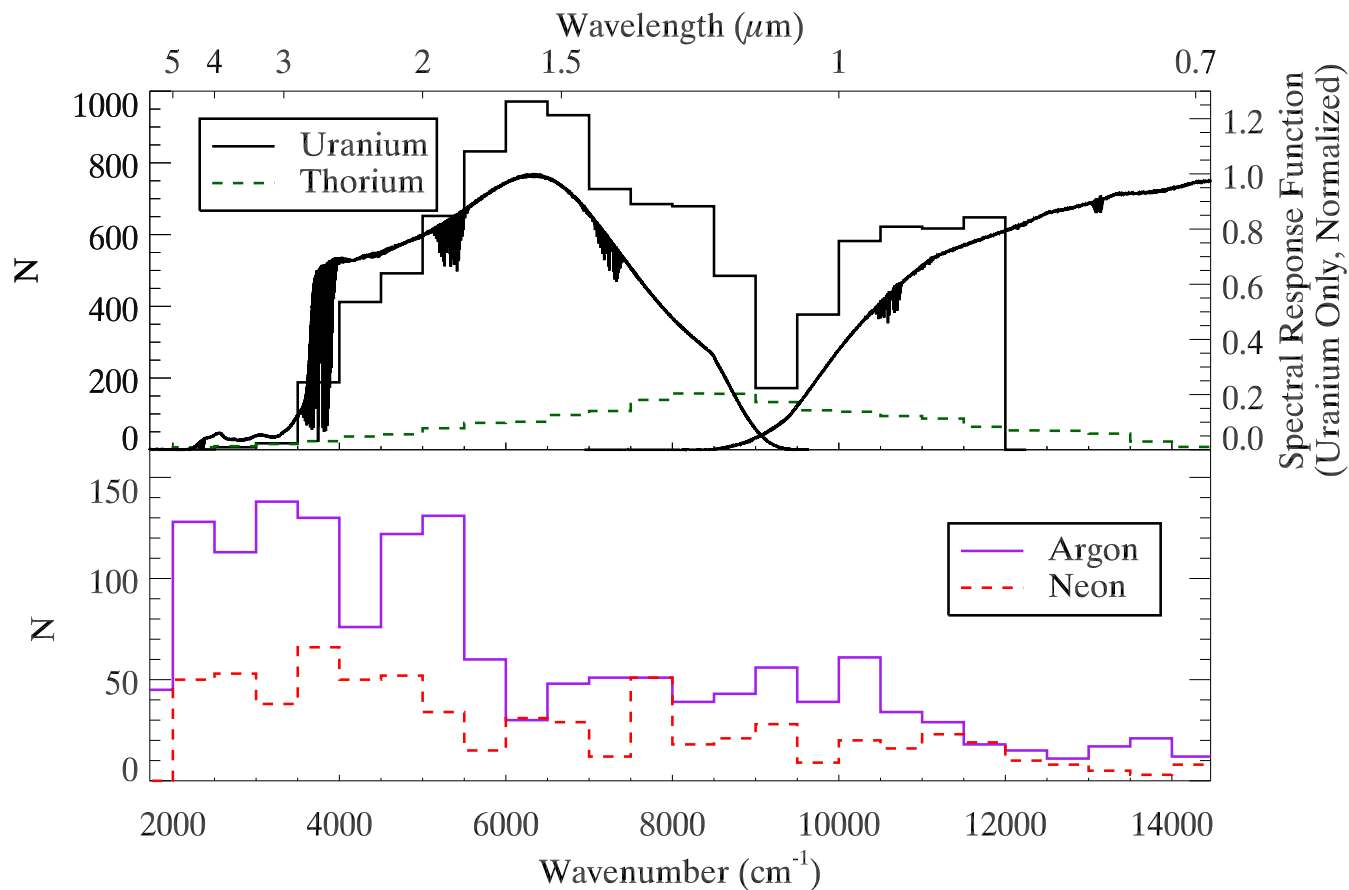


Fig. 6.— Histograms of the number of documented standard uranium, thorium, argon, and neon lines in the NIR. It is important to note that these distributions are not necessarily proportional to the intrinsic distribution density of these spectral lines, since these lines are compiled from various sources and different observation conditions. **Top:** Histograms of the uranium (this work) and thorium (Kerber et al. 2008) lines in the NIR. The large gap in the number of uranium lines around 9250 cm^{-1} is from a gap in the spectral response functions of these archived data. The spectral response function of SP5 (left) and SP3 (right) are based upon tungsten strip lamp spectra taken with the same observing conditions as the U/Ar or U/Ne spectra. The drop in the number of uranium lines above 12000 cm^{-1} is purely artificial, based on our chosen upper-limit for this compilation. **Bottom:** The same, but for argon (Whaling et al. 2002; Sansonetti 2007) and neon standards (Sansonetti et al. 2004).

Table 3: Thorium and Uranium Line Quantities in Astrophysical Bands of the NIR

Band	Wavelength Range (μm)	N_{Th}	N_U
Y	0.9 to 1.1	437	1864
J	1.2 to 1.35	265	1253
H	1.5 to 1.65	94	1175
K	2.0 to 2.4	71	774
L	3.0 to 4.0	18	15
M	4.5 to 5.3	4	0

Notes. A comparison between the number of thorium lines found by Kerber et al. (2008) and the number of uranium lines found in this work. Lines without identifications from this work (indicated with a “?” symbol in the line list) are not accounted for in this table. Note that this is not a comparison between the true number of lines that these two sources provide in these regions, but rather a snapshot of the current number of known lines.